

## Adsorption and Elution Behavior of Cesium and Rubidium on Ammonium Tungstophosphate (AWP)-CaALG Alginate Microcapsules - 9180

Yan Wu, Hitoshi Mimura, Yuichi Niibori,  
Dept. of Quantum Science & Energy Engineering, Graduate School of Engineering, Tohoku University  
Aramaki-Aza-Aoba 6-6-01-2, Sendai, 980-8579 Japan

Chuanpin Lee  
Dept. of Biomedical Engineering and Environmental Sciences, National Tsing Hua University  
101, Section 2, Kuang-Fu Road, HsinChu, 300, Taiwan

Isao Yamagishi, Shinichi Koyama, Masaki Ozawa  
Nuclear Science & Engineering Directorate, Japan Atomic Energy Agency,  
2-4 Shirakata Shirone, Naka-gun, Ibaraki, 319-1195, Japan

### ABSTRACT

Fine crystals of ammonium tungstophosphate (AWP) exchanger having high selectivity toward  $\text{Cs}^+$  were encapsulated in the biopolymer matrices (calcium alginate, CaALG). The characterization of AWP-CaALG microcapsule was examined by scanning electron microscope (SEM), and the uptake and recovery of  $\text{Cs}^+$  and  $\text{Rb}^+$  were investigated by batch and column methods. Spherical and elastic microcapsules were obtained, and the particle size of microcapsules was about 700  $\mu\text{m}$ . A relatively high uptake (%) of  $\text{Cs}^+$  and  $\text{Rb}^+$  above 70% was obtained in the presence of 2.5 M  $\text{HNO}_3$  – 1 M  $\text{NaNO}_3$  solution, and the uptake equilibrium was attained within 5 h. The distribution coefficient of  $\text{Cs}^+$  ( $K_{d,\text{Cs}}$ ) and  $\text{Rb}^+$  ( $K_{d,\text{Rb}}$ ) decreased in the order of coexisting ions,  $\text{H}^+ > \text{Na}^+ \gg \text{NH}_4^+$ . In a wide  $\text{HNO}_3$  concentration range of  $10^{-2}$  - 3 M,  $K_{d,\text{Cs}}$  value for the microcapsule was above  $10^5 \text{ cm}^3/\text{g}$ , while the  $K_{d,\text{Rb}}$  value was around  $500 \text{ cm}^3/\text{g}$  even in the presence of 3 M  $\text{HNO}_3$ . The uptake of  $\text{Cs}^+$  and  $\text{Rb}^+$  followed a Langmuir-type adsorption equation, and the maximum uptake capacity was estimated to be 0.096 and 0.071 mmol/g, respectively. A linear relationship with a slope of about -1 was obtained between  $\log K_d$  and  $\log [\text{NH}_4^+]$  ( $[\text{NH}_4^+] > 0.01 \text{ M}$ ), and the retention volume ( $V_R$ ) values of  $\text{Cs}^+$  and  $\text{Rb}^+$  in chromatography also decreased similarly to the  $K_d$  value. The  $V_R$  value can be predicted from the  $K_d$  value based on the linear relation, and the experimental  $V_R$  values were closed to the calculated ones. Well-resolved chromatogram with resolution ( $R_s$ ) = 1 was obtained by flowing 0.6 M  $\text{NH}_4\text{NO}_3$ . In this case, the total elution percentage of  $\text{Cs}^+$  and  $\text{Rb}^+$  was estimated to be 71% and 83%, respectively. The loaded  $\text{Cs}^+$  and  $\text{Rb}^+$  on column were thus successfully eluted with  $\text{NH}_4\text{NO}_3$  solution, yielding a large difference in  $V_R$  values.

### INTRODUCTION

Recently, much attention has been given to the selective separation and recovery of Cs-137 from high level liquid wastes (HLLWs) in relation to the partitioning of radioactive nuclides and their effective utilization [1-4]. Cesium-137 having relatively long half-life of about 30 years exhibited high radioactivity and heat generation, and large amounts of Cs group (~3.6 kg/1tHU, 45 GWd/t) are contained in HLLWs[5]. Therefore, selective separation of Cs-137 from HLLWs is an important environmental issue for nuclear waste management. In addition, the purified Cs is also expected for the reuse as radiation and heat sources in the field of medicine and industry [6,7].

Many methods for the separation of  $\text{Cs}^+$  such as ion exchange, solvent extraction and co-precipitation

have been studied[8-11]. In the ion-exchange process, heteropolyacids are well known to have selective uptake ability to  $\text{Cs}^+$ . Ammonium tungstophosphate (AWP), a kind of heteropolyacid, which shows a high selectivity toward  $\text{Cs}^+$  and excellent radiation stability, can act as one of the most promising adsorbent for the uptake of  $\text{Cs}^+$ [3, 4]. However, AWP is still not applied to the practical separation process because of its fine powder form which is insufficient for the continuous treatment using packed column. In order to overcome this handling problem, the granulation of AWP powder with alginate gel polymers seems to be one of the most prominent techniques for the practical column operation[3, 4].

Microencapsulation is an unique technique for enclosing active component in a porous polymeric matrix[12-15]. It is well known that alginates (ALG), a kind of biopolymer, has high immobilization ability and this method has been extended to industrial, medical and agricultural fields. Alginate is a salt of alginic acid having carboxyl groups capable to form gels by crosslinking with multivalent metal ions. This immobilizing property of alginate has led to its extensive applications to the microencapsulation of enzymes, subcellular organelles, and living cells[16,17]. Thus, the granulation with alginate gel has several advantages such as simplicity for preparation, mechanical strength and strong acid resistance[12-15].

In this study, we have attempted to encapsulate the fine crystals of AWP exchanger into the biopolymer matrices (calcium alginate, CaALG) by using its high immobilizing ability for the selective separation of  $\text{Cs}^+$  and  $\text{Rb}^+$  from the waste solution containing highly concentrated  $\text{HNO}_3$  and  $\text{NaNO}_3$ . The present paper deals with the preparation of microcapsules (MCs), characterization, uptake properties, and elution properties of  $\text{Cs}^+$  and  $\text{Rb}^+$  for the column packed with MCs.

## **EXPERIMENTAL**

### **Materials**

The AWP exchanger consisting of Keggin-type polyanions ( $\text{PW}_{12}\text{O}_{40}^{3-}$ ) [18] and exchangeable  $\text{NH}_4^+$  ions is used as an active component, and its unit cell composition was  $(\text{NH}_4)_3\text{PO}_4 \cdot 12\text{WO}_3 \cdot 3\text{H}_2\text{O}$  (Wako Pure Chemical Ind.). Sodium alginate (NaALG, 500-600 cP) was purchased from Wako Pure Chemical Ind. The  $\text{Cs}^+$  and  $\text{Rb}^+$  solutions were obtained by diluting the standard solutions ( $10^3$  ppm, Wako Pure Chemical Ind.).

### **Preparation of MCs**

The alginate gel enclosing AWP was prepared as follows. AWP (0.5 g) was kneaded with the NaALG solution ( $50 \text{ cm}^3$ , 1.5 wt%) and fully dispersed by using kneader equipped the function of rotation and revolution. The well-kneaded sol was injected dropwise into a 0.5 M  $\text{Ca}(\text{NO}_3)_2$  solution using a medical needle under constant stirring at room temperature to form MCs. The MCs were stirred gently for one night to enhance the aging. The MCs were then separated from the solution, washed with distilled water and finally air-dried at  $30^\circ\text{C}$  for 2 d. The MCs prepared by gelation of kneaded sols of AWP/NaALG with  $\text{Ca}(\text{NO}_3)_2$  solution were abbreviated as AWP-CaALG.

### **Characterization**

The surface morphology MCs was observed by optical microscope and SEM (Hitachi TM-1000). In order to estimate the acid resistance, the AWP-CaALG specimens (50 mg) were treated with 2.5 M  $\text{HNO}_3$  ( $5 \text{ cm}^3$ ) for 24 h and analyzed by SEM after drying.

### **Determination of Distribution Coefficient ( $K_d$ )**

The distribution of  $\text{Cs}^+$  and  $\text{Rb}^+$  ions for MCs was estimated by batch method. An aqueous solution ( $5 \text{ cm}^3$ ) containing 10 ppm  $\text{Cs}^+$  or  $\text{Rb}^+$  ion was contacted with 50 mg of MCs at  $25 \pm 1^\circ\text{C}$  up to 1 d, which was found to be sufficient for attaining equilibrium. The concentrations of  $\text{Cs}^+$  and  $\text{Rb}^+$  ions were measured by atomic absorption spectrometer (AAS, Jarrell AA890)

The uptake percentage ( $R$ , %) of metal ions removed from the solution and the distribution coefficient ( $K_d$ ,  $\text{cm}^3/\text{g}$ ) are defined as :

$$R = (C_0 - C_t) / C_0 \times 100, \quad (\%) \quad (\text{Eq. 1})$$

$$K_d = ((C_0 - C_f) / C_f) \times V / m, \quad (\text{cm}^3/\text{g}) \quad (\text{Eq. 2})$$

where  $C_0$ ,  $C_t$  and  $C_f$  (ppm) are the concentration of metal ions at initial, at time  $t$ , and at equilibrium, respectively;  $m$  (g) the weight of microcapsules;  $V$  ( $\text{cm}^3$ ) the volume of aqueous phase.

### Column Chromatographic Separation of $\text{Cs}^+$ and $\text{Rb}^+$

The column was prepared by packing about 1.7g of MC in a glass column (5 mm in diameter  $\times$  100 mm long) with thermostatic water jacket. The column volume was estimated to be  $1.8 \text{ cm}^3$ . The  $\text{Cs}^+$  and  $\text{Rb}^+$  ions (250  $\mu\text{g}$ ) were loaded on the upper part of the column, respectively. The eluent used in this study were  $\text{NH}_4\text{NO}_3$  -  $\text{HNO}_3$  solutions. Here, the  $\text{HNO}_3$  was used to restrain the swelling of MCs. The flow rate of eluent was maintained at  $0.14 \text{ cm}^3/\text{min}$ . The effluent was collected by a fraction collector, and concentration of  $\text{Cs}^+$  and  $\text{Rb}^+$  were determined by AAS. The operation runs were carried out at  $25 \pm 1^\circ\text{C}$ .

The elution chromatogram was obtained by plotting the elution percentage (Elution, %) against the elution volume ( $\text{cm}^3$ ). The elution percentage is defined as the ratio of the eluted amount of  $\text{Cs}^+$  or  $\text{Rb}^+$  in each fraction to the initial amount loaded on the column. The retention volume ( $V_R$ ) is defined as the total volume of eluent until the maximum of elution peak, and is given as:

$$V_R = V_m + \rho V_a K_d, \quad (\text{cm}^3) \quad (\text{Eq. 3})$$

where  $V_m$  ( $\text{cm}^3$ ) and  $V_a$  ( $\text{cm}^3$ ) are respectively the interstitial volume and the column volume of adsorbent, and  $\rho$  ( $\text{g}/\text{cm}^3$ ) the density of adsorbent.

The separation parameters such as the number of theoretical plate ( $N$ ), the tailing coefficient ( $S$ ), and the resolution ( $R_s$ ), were defined as follows:

$$N = 16(V_R / W)^2, \quad (\text{Eq. 4})$$

$$S = B/A, \quad (\text{Eq. 5})$$

$$R_s = 2(V_{R,2} - V_{R,1}) / (W_1 + W_2), \quad (\text{Eq. 6})$$

where  $V_R$  is the peak width and the subscript numbers refer to eluted components;  $B$  and  $A$  are respectively the base width of right and left sides of the  $V_R$  value.

## RESULTS AND DISCUSSION

### Surface Morphology and Acid Resistance

**Figures 1(a) and (b)** show the SEM images of the surface of AWP-CaALG. The structure of CaALG gel

matrices is composed of crosslinked polymer networks with ionic bonding of  $\text{Ca}^{2+}$  and carboxyl groups. Obvious spherical and elastic granules were obtained. On the surface of AWP-CaALG, a numbers of fine AWP crystals ( $\sim 1 \mu\text{m}$  in diameter) are seen to be encapsulated. Some creases were observed on the surface of AWP-CaALG. The practical sizes of MCs were estimated to be 0.7 mm in diameter by optical microscope and SEM image. The AWP content in MCs was estimated to be 14 wt%.

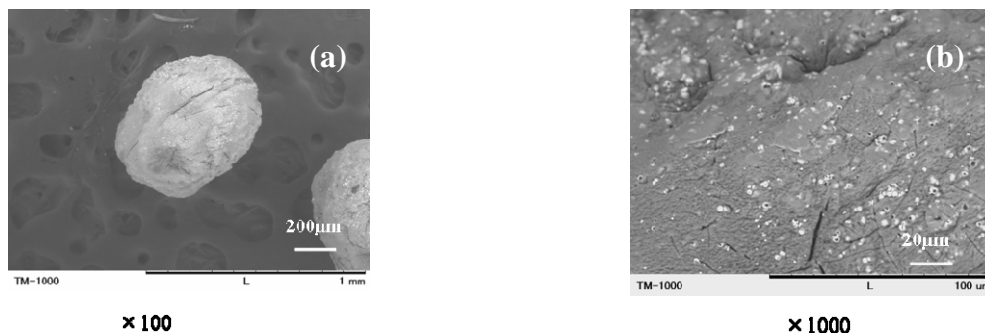


Fig. 1. SEM images of the surface of AWP-CaALG.

The resistance against acid is one of the most important factors for the estimation of chemical stability. **Figures 2(a)** and **(b)** show the SEM images of the surface of AWP-CaALG treated with 2.5 M  $\text{HNO}_3$ . Distinct differences of the surface morphology are observed at higher magnification compared to the fresh AWP-CaALG. The surface of AWP-CaALG treated with acid is apparently more porous than that of the original granule and a number of creases are also observed on the surface. The effect of acid on AWP-CaALG may be realized by the rupturing of the ionic crosslinkage with  $\text{Ca}^{2+}$  ions; the structure of gel matrices treated with  $\text{HNO}_3$  was maintained by the hydrogen bonding of  $\text{H}^+$ /carboxyl group. The treatment of AWP-CaALG with highly concentrated  $\text{HNO}_3$  resulted in the alteration of gel matrices and hence care must be taken in the loss of AWP through the wall of gel matrices in the presence of highly concentrated  $\text{HNO}_3$ .

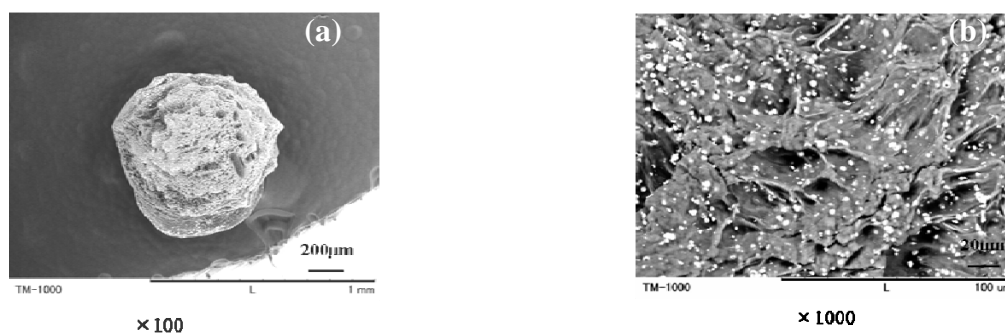
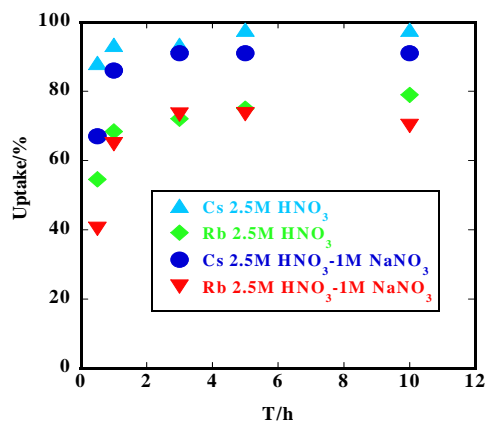


Fig. 2. SEM images of the surface of AWP-CaALG treated with 2.5 M  $\text{HNO}_3$ .

### Uptake Rate

In order to check the equilibration time of  $\text{Cs}^+$  and  $\text{Rb}^+$  for AWP-CaALG, the effect of shaking time on uptake(%) was examined in the presence of 2.5 M  $\text{HNO}_3$  or 2.5 M  $\text{HNO}_3 - 1 \text{ M NaNO}_3$  solutions by batch method (**Fig. 3**). The uptake rates of  $\text{Cs}^+$  and  $\text{Rb}^+$  for MCs in 2.5 M  $\text{HNO}_3$  attained equilibrium rather fast in the initial stages



within 5 h, and relatively large  $R$  value above 70% was obtained. The uptake of  $\text{Cs}^+$  and  $\text{Rb}^+$  in the initial stage was probably due to the adsorption on the surface, followed by a step controlled by mass transfer through gel matrices[19]. On the other hand, in the presence of 2.5 M  $\text{HNO}_3$ – 1 M  $\text{NaNO}_3$ , the initial uptake rates of  $\text{Cs}^+$  and  $\text{Rb}^+$  were tended to decrease. The reason may be due to the swelling of MCs in the presence of highly concentrated  $\text{Na}^+$  ion resulted in the lowering of the uptake rate of  $\text{Cs}^+$  and  $\text{Rb}^+$ .

### Distribution of $\text{Cs}^+$ and $\text{Rb}^+$ in the Presence of Monovalent Cations

Figures 4 (a) and (b) show the  $K_d$  values of  $\text{Cs}^+$  ( $K_{d,\text{Cs}}$ ) and  $\text{Rb}^+$  ( $K_{d,\text{Rb}}$ ) for AWP-CaALG in the presence of different monovalent cations. The  $K_{d,\text{Cs}}$  value was almost constant in the presence of  $\text{HNO}_3$  ( $10^{-3} \sim 3\text{M}$ ). Relatively large  $K_{d,\text{Cs}}$  value above  $10^5 \text{ cm}^3/\text{g}$  was obtained, indicating that AWP-CaALG has strong adsorption ability to  $\text{Cs}^+$ . The  $K_{d,\text{Rb}}$  value was around  $500 \text{ cm}^3/\text{g}$  even in the presence of 3 M  $\text{HNO}_3$ . The uptake of  $\text{Cs}^+$  and  $\text{Rb}^+$  tended to slightly decrease in distribution of  $\text{Cs}^+$  and  $\text{Rb}^+$  shows a linearity with a slope of  $\log K_{d,\text{Cs}}$  and  $\log [\text{NH}_4^+]$ , suggesting that the uptake of  $\text{Cs}^+$  and  $\text{Rb}^+$  or cation-exchange reaction of  $\text{NH}_4^+ \rightleftharpoons \text{Cs}^+$  or  $\text{NH}_4^+ \rightleftharpoons \text{Rb}^+$  or  $\log K_{d,\text{Rb}}$  and  $\log [\text{NH}_4^+]$  was obtained as:

$$\log K_{d,\text{Cs}} = 1.53 - 1.31 \log[\text{NH}_4^+], \quad (\text{Eq. 7})$$

$$\log K_{d,\text{Rb}} = 0.66 - 0.86 \log[\text{NH}_4^+]. \quad (\text{Eq. 8})$$

Thus, the calculated  $V_R$  values of  $\text{Cs}^+$  and  $\text{Rb}^+$  can be defined by substituting Eq. 7 or Eq. 8 into Eq. 3. The  $K_{d,\text{Cs}}$  and  $K_{d,\text{Rb}}$  decreased in the order of coexisting ions,  $\text{H}^+ > \text{Na}^+ \gg \text{NH}_4^+$ . This result was similar to that of decreasing order of the size of hydrated cations[21]. The effect of  $\text{NH}_4^+$  on the uptake for MCs indicated that the chromatographic separation of  $\text{Cs}^+$  and  $\text{Rb}^+$  can be achieved by controlling the concentration of  $\text{NH}_4^+$ .

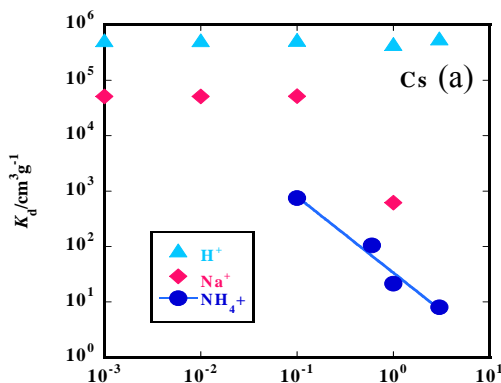


Fig. 3. Effects of shaking time on the uptake(%) of  $\text{Cs}^+$  and  $\text{Rb}^+$ .  $V/m$ :  $100 \text{ M cm}^3/\text{g}$ ; 10 ppm  $\text{Cs}^+$  and  $\text{Rb}^+$ ; 2.5 M  $\text{HNO}_3$ ; 2.5 M  $\text{HNO}_3$ -1M  $\text{NaNO}_3$ ;  $25^\circ\text{C}$ .

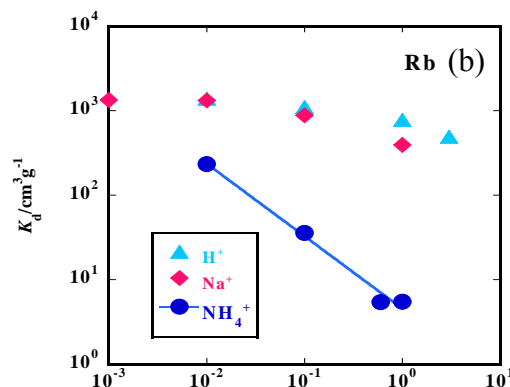


Fig. 4. Effects of monovalent cation concentration on  $K_{d,\text{Cs}}$  and  $K_{d,\text{Rb}}$ .  $V/m=100 \text{ cm}^3/\text{g}$ ; 10 ppm  $\text{Cs}^+$  and  $\text{Rb}^+$ ;  $25^\circ\text{C}$ , 1 d.

The uptake isotherm of  $\text{Cs}^+$  for AWP-CaALG was obtained in a wide range of initial  $\text{Cs}^+$  concentration from 10 ppm to 800 ppm. The equilibrium amount of  $\text{Cs}^+$  adsorbed on AWP-CaALG approached a constant value with increasing concentration, suggesting that the uptake of  $\text{Cs}^+$  follows a Langmuir-type adsorption equation [22]. The Langmuir equation

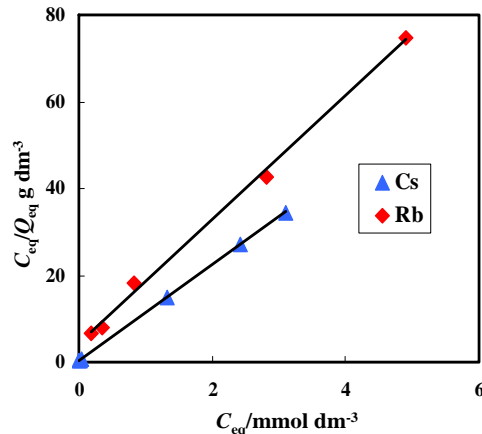


Fig. 5. Langmuir-plots of  $\text{Cs}^+$  and  $\text{Rb}^+$  uptake for AWP-CaALG. 2.5 M  $\text{HNO}_3$ -1M  $\text{NaNO}_3$ ;  $25^\circ\text{C}$ ; 1d.

can be rewritten as follows:

$$C_{\text{eq}}/Q_{\text{eq}} = 1/KQ_{\text{max}} + (1/Q_{\text{max}})C_{\text{eq}} \text{ (g/dm}^3\text{)}, \quad (\text{Eq. 9})$$

where  $C_{\text{eq}}$  (mol/dm<sup>3</sup>) and  $Q_{\text{eq}}$  (mol/g) are the equilibrium concentrations of Cs<sup>+</sup> in the aqueous and solid phases, respectively;  $Q_{\text{max}}$  (mol/g) is the maximum amount of Cs<sup>+</sup> taken up;  $K$  (dm<sup>3</sup>/mol) is the Langmuir constant.

As seen in **Fig. 5**, a fairly linear relation between  $C_{\text{eq}}/Q_{\text{eq}}$  and  $C_{\text{eq}}$  was obtained from Langmuir-plots for AWP-CaALG. The result shows that the  $Q_{\text{max}}$  value of Cs<sup>+</sup> for AWP-CaALG was estimated to be 0.096 mmol/g. The uptake of Rb<sup>+</sup> also followed a Langmuir adsorption isotherm, and the  $Q_{\text{max}}$  value of Rb<sup>+</sup> was estimated to be 0.071 mmol/g.

### Chromatographic Separation of Cs<sup>+</sup> and Rb<sup>+</sup>

Chromatographic separation was examined by varying the concentration of eluting reagent of NH<sub>4</sub>NO<sub>3</sub> (0.6 – 3 M) -1 M HNO<sub>3</sub>. **Figures 6 (a) ~ (c)** show the chromatograms obtained at different concentrations of NH<sub>4</sub>NO<sub>3</sub> and their elution data are summarized in **Table I** and **II**.

**Figure 6(a)** illustrates the chromatogram of Cs<sup>+</sup> and Rb<sup>+</sup> eluted with 0.6 M NH<sub>4</sub>NO<sub>3</sub>-1 M HNO<sub>3</sub>. Well-resolved chromatogram with the resolution ( $R_s$ ) = 1 was obtained. A sharp elution curve of Rb<sup>+</sup> having  $N=24$  was obtained, yielding the  $V_R$  value of 16 cm<sup>3</sup> which was close to the calculated one. The Cs adsorbing on AWP-MC was gently eluted from the column yielding the  $N=7.3$  and larger  $V_R$  value of 87 cm<sup>3</sup>. The recovery of Cs<sup>+</sup> and Rb<sup>+</sup> was estimated to be 71% and 83%, respectively.

**Figures 6 (b)** and **(c)** show the elution chromatograms with 1 M NH<sub>4</sub>NO<sub>3</sub>-1 M HNO<sub>3</sub> and 3 M NH<sub>4</sub>NO<sub>3</sub>-1 M HNO<sub>3</sub>, respectively. The  $R_s$  were calculated to be 0.62 and 0.16 at 1 and 3 M NH<sub>4</sub>NO<sub>3</sub>, respectively. A relatively sharp and symmetric profile was observed in the elution

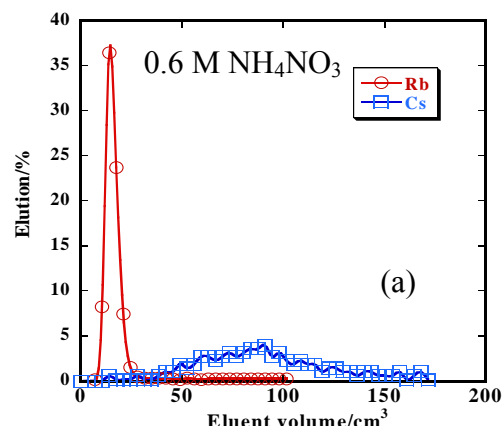


Fig. 6(a). Chromatographic separation of Cs<sup>+</sup> and Rb<sup>+</sup> through AWP-CaALG column. AWP-CaALG: 1.7 g; Cs<sup>+</sup>:200 μg; Rb<sup>+</sup>: 200 μg; eluent: 0.6 M NH<sub>4</sub>NO<sub>3</sub>-1 M HNO<sub>3</sub>; flow rate: 0.14 cm<sup>3</sup>/min; 25°C.

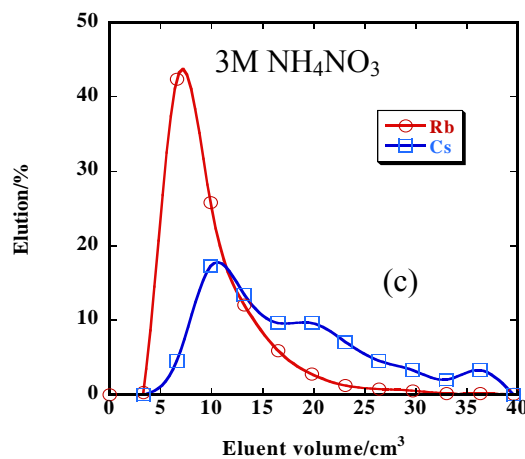
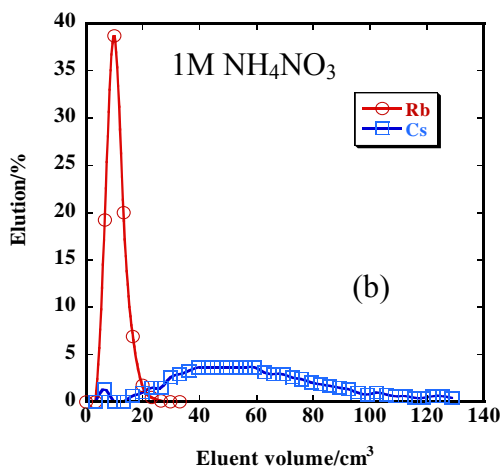


Fig. 6(b) and (c). Chromatographic separation of  $\text{Cs}^+$  and  $\text{Rb}^+$  through AWP-CaALG column. AWP-CaALG: 1.7 g;  $\text{Cs}^+$ :200  $\mu\text{g}$ ;  $\text{Rb}^+$ : 200  $\mu\text{g}$ ; eluent: 1 M  $\text{NH}_4\text{NO}_3$ -1 M  $\text{HNO}_3$ , 3 M  $\text{NH}_4\text{NO}_3$ -1 M  $\text{HNO}_3$ ; flow rate: 0.14  $\text{cm}^3/\text{min}$ ; 25°C.

curve of  $\text{Rb}^+$ , suggesting that the  $\text{Rb}^+$  was readily eluted with  $\text{NH}_4\text{NO}_3$ . The increase in  $\text{NH}_4\text{NO}_3$  concentration resulted in a shift of each elution curve to lower effluent volumes, and the  $V_R$  value of  $\text{Cs}^+$  and  $\text{Rb}^+$  in chromatography was lowered similarly to the  $K_d$  value. The  $N$  value was tended to decrease with increasing the concentration of  $\text{NH}_4\text{NO}_3$ . The  $S$  value was estimated to be 1.5 ~ 3.7, indicating a slight tailing in the chromatogram(**Table I** and **II**). In this case, the elution percentage was estimated to be above 70%.

Thus, the lowering of  $\text{NH}_4^+$  concentration resulted in an enhancement of  $R_s$  value. The chromatographic separation of  $\text{Cs}^+$  and  $\text{Rb}^+$  was successfully accomplished by using the eluent of 0.6 M  $\text{NH}_4\text{NO}_3$ . In order to enhance the  $R_s$  and elution percentage, lower flow rate, smaller particle size and longer column are required for the practical operation.

Table I. Elution Data of  $\text{Cs}^+$  with  $\text{NH}_4\text{NO}_3$  Solutions

$\text{NH}_4\text{NO}_3/\text{M}$	$V_R/\text{cm}^3$	$t_R/\text{min}$	$N$	$S$	Elution/%	Calculated $V_R/\text{cm}^3$	$R_s$
0.6	87	670	7.3	0.9	71	117	1.0
1	46	351	3.5	1.5	70	59	0.62
3	24	185	2.5	3.4	75	16	0.16

Table II. Elution Data of  $\text{Rb}^+$  with  $\text{NH}_4\text{NO}_3$  Solutions

$\text{NH}_4\text{NO}_3/\text{M}$	$V_R/\text{cm}^3$	$t_R/\text{min}$	$N$	$S$	Elution/%	Calculated $V_R/\text{cm}^3$	$R_s$
0.6	16	124	24	1	83	15	1.0
1	11	85	11	1.8	87	11	0.62
3	9	71	4.4	3.7	92	6	0.16

## CONCLUSIONS

The uptake properties of  $\text{Cs}^+$  and  $\text{Rb}^+$ , characterization and dynamic adsorption properties were investigated by using AWP-CaALG. The uptake of  $\text{Cs}^+$  and  $\text{Rb}^+$  for AWP-CaALG was fairly fast in the initial stage and the uptake equilibrium attained within 5 h. The  $K_{d, \text{Cs}}$  for AWP-CaALG was almost constant ( $10^5 \text{ cm}^3/\text{g}$ ) up to 3 M  $\text{HNO}_3$ . The  $K_{d, \text{Cs}}$  and  $K_{d, \text{Rb}}$  decreased in the order of coexisting ions,  $\text{H}^+ > \text{Na}^+ \gg \text{NH}_4^+$ . The uptake isotherm of  $\text{Cs}^+$  and  $\text{Rb}^+$  followed a Langmuir-type adsorption equation. The adsorbed  $\text{Cs}^+$  and  $\text{Rb}^+$  can be successfully eluted with the  $\text{NH}_4\text{NO}_3$ , yielding an excellent peak resolution ( $R_s=1$ ). The MCs enclosing AWP were thus effective for the selective separation and recovery of  $\text{Cs}^+$  and  $\text{Rb}^+$ .

## REFERENCES

1. Technical Report Series, No. 356, IAEA, Vienna, Austria (1993).
2. H. Mimura, M. Saito, K. Akiba and Y. Onodera, *Solvent Extr. Ion Exch.*, **18**(5), pp. 1015-1027(2000).
3. H. Mimura, M. Saito and K. Akiba, *J. Nucl. Sci. Technol.*, **38**, No. 10, pp. 872-878(2001).
4. H. Mimura and Y. Onodera, *J. Nucl. Sci. Technol.*, **39**, No. 3, pp. 282-285(2002).
5. R. Ando and T. Takano, JAERI-Research 99-004(1994).
6. H. Mimura and K. Akiba, *J. Nucl. Sci. Technol.*, **33**, No. 6, pp. 511-518(1996).
7. H. Mimura, K. Iijima and K. Akiba, *J. Nucl. Sci. Technol.*, **34**, No. 3, pp. 269-276(1997).
8. R. P. Buch and G. J. K. Acres, AERE-R-12830(1987).
9. M. L. Dietz, E. P. Horwitz, S. Rhoads, R.A. Bartsch and J. Krzykawski, *Solvent Extr. Ion Exch.* **14**, 1, pp.1-12(1996).
10. R. Chiarizia, E. P. Horwitz, R. A. Bauvais and S. D. Alexandratos, *Solvent Extr. Ion Exch.*, **16**, 3, pp. 875-898(1998).
11. A. F. Reguillon, B. Dunjic, M. Lemaiue , and R. Chomel, *Solvent Extr. Ion Exch.*, **19**, 1, pp. 181-191(2001).
12. H. Mimura, T. Sakakibara, Y. Niibori and K. Tanaka, *J. Ion Exchange*, **16**, pp. 29-33(2005).
13. M. Outokesh, H. Mimura, Y. Niibori and K. Tanaka, *Ind. & Eng. Chem. Res.*, **45**, pp. 3633-3643(2006).
14. Y. Wu, H. Mimura and Y. Niibori, *J. Ion Exchange*, Vol. **18**, No. **4**, pp. 396-401(2007).
15. Y. Wu, M. Outokesh, H. Mimura and Y. Niibori, *Progress in Nuclear Energy*, **50**, pp. 487-493(2008).
16. H. Watari and S. Hatakeyama , *Analytical Science*, **7**, pp. 487-489(1991).
17. E. Kamio and K. Kondo, *Journal of Chemical Engineering of Japan*, **35**, pp. 574-581 (2002).
18. J. F. Keggin, Roc. Roy. Soc., London, A144, 75(1934).
19. F. Sebesta, J. John and A. Motl, IAEA-TECDOC-947, Vienna, Austria, p.79(1997).
20. V. Pekarek and V. Vesely, *Talanta*, **19**, 11, pp.1285-1293(1972).
21. H. A. Laitinen and W.E. Harris, "Chemical Analysis", McGraw-Hill Kogakusha, Ltd., Tokyo, p.14(1975).
22. P. Benes and V. Majer, "Trace Chemistry of Aqueous Solutions", Elsevier Scientific Publishing Company, Amsterdam, p. 199(1980).